Chinese Journal of Mechanical Engineering: Additive Manufacturing Frontiers 1 (2022) 100012

Contents lists available at ScienceDirect

Chinese Journal of Mechanical Engineering: Additive Manufacturing Frontiers

journal homepage: www.elsevier.com/locate/cjmeamf

# Additive Manufacturing of Ceramics from Liquid Feedstocks

Giorgia Franchin[a], Hamada Elsayed[a,b], Renata Botti[a], Kai Huang[a], Johanna Schmidt[a], Giulio Giometti[a], Alice Zanini[a], Anna De Marzi[a], Marco D'Agostini[a], Paolo Scanferla[a], Yurun Feng[a], Paolo Colombo[a,c,*]

[a] Dipartimento di Ingegneria Industriale, Università di Padova, via Marzolo 9, 35131 Padova, Italy
[b] Refractories, Ceramics and Building Materials Department, National Research Centre, El Buhouth Str., 12622 Cairo, Egypt
[c] Department of Materials Science and Engineering, Pennsylvania State University, University Park, PA 16802, USA

ARTICLE INFO

*Keywords:*
Additive manufacturing
Preceramic polymers
SiOC

ABSTRACT

In this review, we summarize the research activities carried out by our research group at the University of Padova on the additive manufacturing of ceramics from liquid feedstocks. Particularly, we evaluate the use of preceramic polymers, geopolymers, and sol-gel solutions. We mainly focus on processing with liquid feedstocks because they have some advantages with respect to slurry-based feedstocks in which powders are present. Particularly, lower viscosity, enhanced transparency, and lack of scattering and sedimentation are advantageous features for vat photopolymerization processes, whereas the absence of particulates reduces clogging problems at the nozzle for extrusion-based processes. Simultaneously, preceramic polymers and geopolymers have some limitations in terms of the range of ceramic compositions that can be obtained; sol-gel solutions are intrinsically unstable, whereas printed objects suffer from drying issues. Nevertheless, we successfully produced high-quality parts using a variety of additive manufacturing techniques, some of which (e.g., volumetric additive manufacturing) have been proposed for the fabrication of ceramic components for the first time.

## 1. Introduction

Particle-based feedstocks, either in the form of powders or as a slurry with variable liquid content, have been the norm for the fabrication of ceramic components by additive manufacturing (AM), followed by de-binding and sintering steps [1,2]. Technology such as binder jetting (BJ) relies on the layer-by-layer deposition of a powder bed, on which the shape of the desired component is inscribed by jetting a suitable liquid binder. A similar approach was adopted by selective laser melting/melting (SLS/SLM), in which the powder was selectively sintered/fused together using a laser beam. Direct ink writing (DIW) extrudes through a nozzle with a thick paste that should have a specific rheology to enable the fabrication of parts possessing overhangs and unsupported features. Stereolithography (SLA) or digital light processing (DLP) employs a slurry whose viscosity is controlled by the amount of powders dispersed, and it must be adapted to the specific technology used (i.e., DLP printer with a bottom-up or top-down configuration). Two-photon polymerization (TPP) enables the fabrication of parts with sub-micron resolution, thereby limiting its use to slurries containing nano-sized particles, which should also be highly diluted to provide the required optical transparency. A similar situation occurs for inkjet printing (IP), where the small particle size and dilution serve the purpose of avoiding the clogging of the nozzle. The feedstocks used for fused deposition modeling (FDM) and laminated object manufacturing (LOM) are in a separate category because they rely on a continuous thermoplastic filament or tapes, respectively, and therefore, not on a material containing loose particles.

However, considering the fact that a high powder loading is generally desirable to reduce sintering shrinkage, particle-based feedstocks have many drawbacks. For example, concerning vat photopolymerization technologies, the slurry is often too viscous to spontaneously form a new layer that should be irradiated and therefore requires special printers with a built-in mechanism (rotating blade, doctor's blade), forcing its fast spreading. These printers are considerably more expensive than currently available common DLPs. Another issue is the light scattering caused by the particles, which often possess a different (higher) refractive index from the surrounding photopolymer. This interferes with the photopolymerization reaction, leading to reduced reactivity and printing precision. Additionally, dark or radiation-absorbing particles, such as SiC or $Si_3N_4$, require a high-intensity light source, and the maximum layer thickness is limited, leading to lengthy printing times. Moreover, the stabilization of particles in the non-aqueous medium is difficult, especially if the particle density is high. Therefore, obtaining a suitable viscosity at high particle loading is therefore not simple. Recent devel-

* Corresponding author.
*E-mail address:* paolo.colombo@unipd.it (P. Colombo).

https://doi.org/10.1016/j.cjmeam.2022.100012
Received 19 October 2021; Received in revised form 20 January 2022; Accepted 8 February 2022
Available online 16 February 2022

**Table 1**
Comparison of conventional ceramic slurries and preceramic polymer-based inks for vat photopolymerization technologies, with focus on their viscosity and cure sensitivity.

| Ceramic material | Particle size ($\mu$m) | Surface area ($m^2/g$) | Solid fraction (vol%) | Viscosity(mPa•s) | Cure sensitivity ($\mu$m) | Ref. No. |
|---|---|---|---|---|---|---|
| Hydroxyapatite | 1 | 2.1 | 52 | 2870 | 50.7 | [4] |
| $BaTiO_3$ | 0.5 | 2.3 | 40 | 230 | 32.9 | [5] |
| Alumina | 0.4 | 4.1 | 40 | 200 | 52 | [6] |
| Alumina + Zirconia 3Y 3:1 wt | 0.4–0.2 | – | 40 | 380 | 34.7 | |
| Cordierite | 0.35 | – | 40 | 1490 | 113.2 | [7] |
| Zirconia 3Y | 0.385 | 9 | 40 | 2900 | 49 | [8] |
| Ceramic material | Preceramic polymer fraction (wt%) | Preceramic polymer | Cerami yield (wt%) | Viscosity (mPa•s) | Cure sensitivity ($\mu$m) | Ref. No. |
| SiOC | 40 | SILRES MK | 33 | 446 | 250 | [9] |
| | 53 | IC836 | 39 | 399 | | |
| | 53 | 604 | 42 | 395 | | |
| SiOC + metal NPs | ~ 70 (after solvent removal) | SILRES MK + MEMO Zr- and T-alkoxides | 44 | 100 | 200 | [10] |

opments and perspectives on the photopolymerization AM of ceramics have been reported in a recent systematic review [3].

Concerning DIW, the dimensions of the powders control the dimensions of the nozzle that can be successfully used for the extrusion of the paste. Therefore, the dimension of the minimum feature achievable in the part, its surface quality, the clogging of the nozzle, and drying of the ink are common issues leading to macro-defects in the printed components.

The use of all-liquid feedstocks can solve some of the above issues, providing higher flexibility in terms of the processing and quality of prints. All-liquid systems include preceramic polymers, sol-gel formulations, and geopolymers. The latter starts as a slurry, comprising an aluminosilicate solid phase and an alkaline activating solution, but the solid quickly disappears and is dissolved into the reactive high-pH medium.

Table 1 presents the selection of conventional ceramic suspensions and preceramic polymer-based inks (as an example for liquid-based systems) employed for vat photopolymerization, where significant advantages in the viscosity and curing behavior can be recognized. Cure sensitivity $D_p$ is reported as it is an intrinsic property of photocurable feedstock derived from the cure depth equation [11]

$$C_d = D_p \ln \frac{E}{E_c},$$

where $C_d$ is the cure depth, $E$ is the energy intensity provided by the equipment, and $E_c$ is the critical energy intensity required for photopolymerization.

Despite their advantages, one must first recognize that not all of the potential liquid feedstocks can be used with every class of AM technology, and that the compositional range of the resulting ceramics is rather limited for all but the sol-gel formulations, because preceramic polymers are mainly based on Si-containing compounds [12].

This paper does not intend to review the entire work published on the subject but rather to summarize and illustrate the research carried out by the authors, which, in many cases, paved the way for additional investigation and development by other scientists.

## 2. Preceramic Polymer-based Feedstocks

Preceramic polymers such as siloxanes, silazanes, and carbosilanes have been tested as feedstocks for most AM technology categories, including binder jetting, inkjet printing, laminated object manufacturing, vat photopolymerization (digital light processing and two-photon polymerization), and fused deposition modeling [12,13]. Binder jetting requires a particle-based feedstock [1,2,14–16], whereas fused deposition modeling uses a filament [17,18]; therefore, these technologies have not been included in this review.

In our research, we mainly employed commercially available silicone resins because of their widespread availability, ease of processing, and variable composition (in terms of the C content in the resulting SiOC ceramic), making them of interest for a wide range of potential applications. However, we also 3D printed silazane-based components using both the DLP and DIW technologies.

It should be noted that in most cases, cross-linking the preceramic polymer is necessary before pyrolysis to retain the shape of the printed component upon heating. Furthermore, when fabricating a component using a preceramic polymer, a high ceramic yield (>60 wt%) is preferred to reduce the shrinkage and potential cracking issues related to the pyrolysis process.

### 2.1. Vat photopolymerization

To generate a solid structure through the photopolymerization process, a material containing photoreactive moieties is required, in addition to a photoinitiator and, if desired, a photoabsorber for controlling the penetration of the radiation in the $z$-direction. Five different approaches can be used to process preceramic polymers via vat photopolymerization, maintaining a suitably high ceramic yield.

- Using commercially available preceramic polymers containing reactive groups (e.g., acrylic, vinyl, or epoxy groups). However, they typically either have a low ceramic yield (e.g., <10 wt% for siloxane acrylates), because their molecular structure has not been designed to provide a high amount of inorganic residue upon pyrolysis, or are subject to sluggish reactions, making printing inconveniently slow (e.g., vinyl siloxanes, see also 3).
- Synthesis of preceramic polymers with high ceramic yields and suitable photocurable groups. This requires appropriate chemical knowledge and is often limited to lab-based developments [19];
- Building a preceramic polymeric structure starting from the photoinduced reaction of two distinct (monomeric, oligomeric, polymeric) precursors (thiol-ene click chemistry can be successfully used, but it carries S and O contaminants) [20–23];
- Chemically modifying a commercially available, high-ceramic-yield preceramic polymer by grafting photocurable moieties [24,25];
- Blending of a photocurable polymer with a non-photocurable, high-ceramic yield, commercially available preceramic polymer. In this case, no crosslinking reaction between the two polymers occur upon light illumination, and the preceramic polymer does not need to have specific functional moieties.

From an engineering point of view, the most favorable approaches are #4 and #5, which take advantage of existing, well-proven, and available materials, and require limited chemical skills and equipment. Therefore, these were evaluated in our laboratory.

The first example of a ceramic component printed using the vat photopolymerization technique (DLP) and a preceramic polymer was

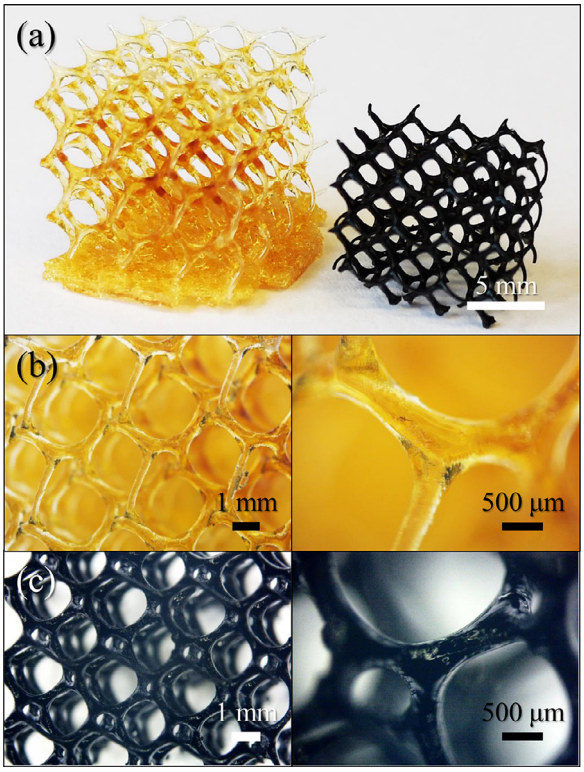


**Fig. 1.** An example of a highly porous structure (~96 vol.% porosity) obtained using this approach: (a) Digital images of a cellular structure before and after pyrolysis printed by DLP using a chemically modified preceramic polymer; (b) images of the as-printed and (c) pyrolyzed SiOC component.

published online on November 6, 2015, by Zanchetta et al [26], in which an acrylate silicon-containing precursor (trimethoxysilyl) propyl-methacrylate (TMSPM) was hydrolyzed and catalytically reacted with the Si-OH moieties of a silicone resin (MK, Wacker Chemie, Germany) to form a liquid photocurable precursor. A 20 wt% acrylate was sufficient to obtain a solution with an appropriately low viscosity that was capable of being printed using a limited exposure time (< 2 s). The ceramic yield of the printed material was of the order of 70 wt% (when the low-volatility solvent was fully evaporated before pyrolysis), yielding fully dense structures with ~25% linear shrinkage. Remarkably, considering that the silicone resin has a glass transition temperature (Tg) of ~50°C, no softening of the printed structure occurred during pyrolysis. Evidently, the organic moieties bridging the siloxane chains contributed to avoiding viscous (and viscoelastic) deformation caused by the gravitational forces acting on the softened material above its Tg because their decomposition occurs at a temperature higher than that triggering the thermal cross-linking of the residual Si-OH moieties of the silicone resin (~150–180°C). An example of a highly porous structure (~96 vol.% porosity) obtained using this approach is shown in Fig. 1.

The idea of merely blending a non-photocurable, high-ceramic-yield preceramic polymer with a photocurable polymer is simple but not straightforward. In addition to issues such as finding a common solvent (necessary for dissolving the preceramic polymer, if solid, or controlling the viscosity of the system) and controlling the phase separation between the two polymers, the possibility of trapping the liquid preceramic polymer within the polymer crosslinked by photocuring without loss of material after cleaning the printed part is not presented. Furthermore, during pyrolysis, the un-crosslinked preceramic polymer starts to soften and flow; therefore, it must be appropriately supported by the photocured polymer to retain its shape and avoid bloating. Although the process can be extended to all different classes of preceramic polymers, we tested different siloxane materials and found that silicone resins containing phenyl groups were the most compatible with the photocurable polymers employed (e.g., silicone resins Silres 601 and H44, Wacker Chemie, Germany) [27]. The amount of photocurable polymer in the blend controls the printing time as well as the ceramic yield and shrinkage upon pyrolysis; the first two parameters decrease while the latter increases with increasing content. It should be stressed that, in most cases, it is better to achieve a high ceramic yield. Having a large amount of low-to-zero ceramic yield photocurable polymer in the formulation could be a highly useful strategy for the realization of ceramic components with a resolution that is not achievable using certain additive manufacturing technology. For instance, if a DLP printer usually has a resolution limit in the *x-y* plane of 50 µm, with 25% linear shrinkage upon heating, the minimum feature size achievable after pyrolysis is ~37.5 µm. If the linear shrinkage of the printed part is much higher (e.g., 70%) because of the presence of a large amount of a low-to-zero ceramic yield polymer in the system, then the printing resolution is significantly increased.

SiOC parts several centimeters in size and possessing very complex architectures controlling their mechanical behavior, could also be produced using this approach [28]. Moreover, we demonstrated that this blending approach can be carried out using either a low-ceramic-yield (7 wt%) photocurable silicone (TEGO RC 711, Evonik Industries, Germany) [26,27] or a fully organic photocurable polymer (examples include Industrial Blend, Fun to do, The Netherlands), with ~0 wt% ceramic yield [29].

Remarkably, amounts as high as ~80 wt% of the high-loss photocurable polymer can be present in the blends and still facilitate the formation of a solid ceramic part after pyrolysis, indicating that the phase separation between the organic polymer and silicone resin must generate two continuous interconnected phases. Moreover, after pyrolysis, the parts were fully dense, suggesting that the decomposition of the organic resin occurs in a suitable range of temperatures (~350–500 °C) for, on one hand, avoiding the collapse of the structure due to the softening of the preceramic polymer and, on the other hand, enabling the full elimination of the decomposition gases upon pyrolysis. Interestingly, the surface quality of the parts after cleaning away the residual feedstock solution with isopropanol was very good. The lack of macro-defects, such as pinholes, indicates that the solvent was not capable of extracting the un-crosslinked preceramic polymer from the structure. 3D printed, high carbon-containing SiOC ceramics were produced using this approach, which can be employed in electromagnetic microwave absorption applications [29]. An example of the fabricated SiOC structure is shown in Fig. 2.

Finally, it should also be stressed that using blends of preceramic polymers and low-to-zero ceramic yield photopolymers enables the fabrication of defect-free ceramic components, in which the maximum feature size exceeds that achievable using a pure preceramic polymer. Typically, the maximum size that can be obtained when pyrolyzing a preceramic polymer without any fillers is of the order of a maximum of a few hundred microns. Using this approach, parts as thick as a few millimeters could be produced without cracks or voids, suggesting that the release of the decomposition gases from the preceramic polymer was favored by the presence of a residual network of interconnected pores derived from the elimination of the photopolymer.

We also evaluated the additive manufacturing of ceramic components using the two-photon polymerization technique and a commercial solvent-free acrylate siloxane (TEGO RC 711, Evonik Industries, Germany), with a suitable photopolymerization initiator [30]. The micron-scale parts with submicron resolution were printed on a fused silica slide after developing a nonstandard printing configuration and optimizing the processing conditions. To eliminate the shape distortions that occur during pyrolysis owing to the constrained shrinkage of the printed parts attached to a solid substrate, they were printed on supports made of the same preceramic polymer. By adjusting the dimensions of the supporting pillar with respect to those of the printed component, it was possible to fabricate undistorted SiOC structures (see Fig. 3(a)). Furthermore, to overcome the limitation of TPP, which requires a part to

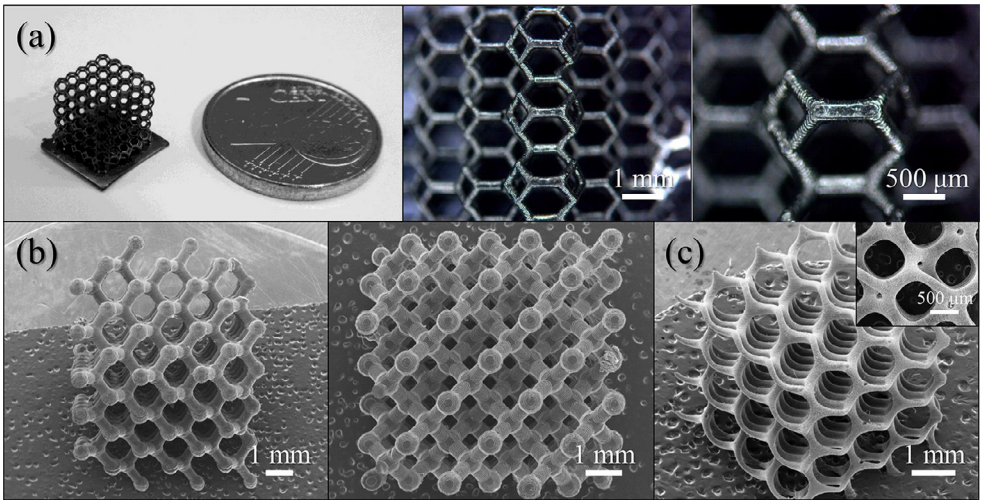


**Fig. 2.** An example of the fabricated SiOC structure: (a) Digital images of a SiOC pyrolyzed Kelvin structure printed by DLP using a preceramic and photocurable polymer blend; SEM images of (b) a SiOC pyrolyzed diamond and (c) a SiOC cellular structure.

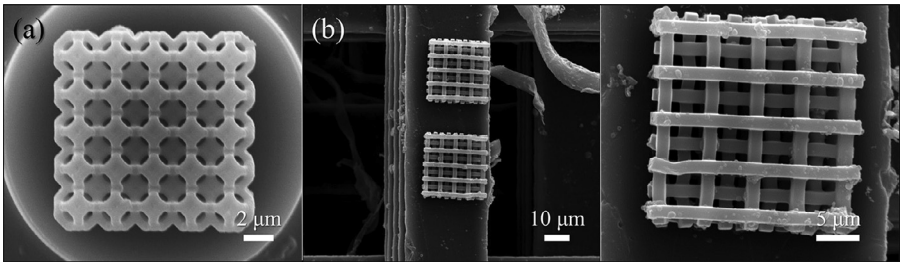


**Fig. 3.** SEM images of (a) a pyrolyzed SiOC Kelvin structure printed by TPP, and (b) a SiOC pyrolyzed log-pile structure produced using a hybrid vat polymerization technology (DLP+TPP).

be fabricated on a support from which it cannot be easily removed, we developed a hybrid additive manufacturing process combining in-series DLP and TPP. Particularly, DLP enables the fabrication of macro-sized (a few centimeters), free-standing components but with a limited size resolution of a few tens of microns, whereas TPP has a sub-micron resolution but can only produce parts with dimensions of a few millimeters that are connected to a substrate. By combining the two technologies, multiscale, free-standing ceramic components that can be easily handled and possess a feature size resolution that is not achievable by solely using DLP were fabricated [31]. As a demonstration of this concept, we first printed a mm-sized log-pile scaffold using DLP and then printed the same structure on top of it using TPP. The use of the same preceramic polymer in both technologies enabled the avoidance of any distortion derived from differential shrinkage (see Fig. 3(b)). We envision those useful structures, such as nozzles or needles with a uniquely small and precise tip shape, can be fabricated using this approach.

Provided that special equipment is used, vat photopolymerization technologies can enable volumetric printing, that is, the growth of a cross-linked solid object within a liquid vat instead of on its surface. This results in several advantages over conventional layer-based printing methods, namely, a higher processing speed and the ability to print into highly viscous fluids, eliminating the need for support structures [32,33]. For the first time, we tested the use of a photocurable preceramic polymer solution with a novel linear volumetric 3D printing process referred to as xolography, in which complex objects are manufactured using two intersecting light beams of different wavelengths to solidify localized regions that are stabilized by the surrounding viscous fluid matrix. Specifically, the process employs dual-color photopolymerization, in which curing is mediated by a two-color photoinitiator added to the resin, which is activated by the first radiation with a wavelength in the UV region, whereas the absorption of the second radiation (with a wavelength in the visible range) initiates photopolymerization via the formation of radicals. No support structures for overhanging features are required, and printing rates of up to ~1 $cm^3/s$ with a resolution of 10–50 µm, are possible [33].

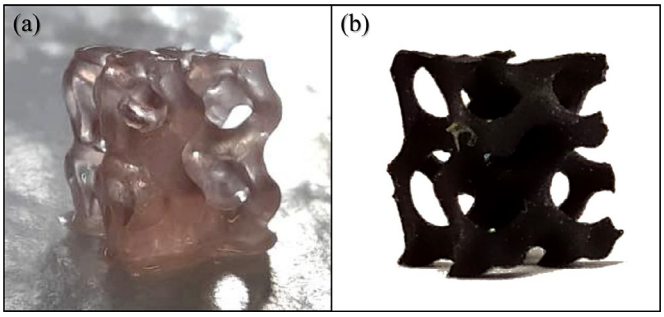


**Fig. 4.** Optical images of a 3D printed structure obtained by xolography: (a) after printing; (b) after pyrolysis.

To fulfil the specific technology requirements, we had to tailor the viscosity, transparency, and reactivity of the feedstock, which contained silicone resin (H44, Wacker Chemie, Germany). Despite these being only the first attempts, we successfully fabricated a gyroid structure (see Fig. 4), demonstrating that this approach is very promising for the rapid volumetric production of ceramic parts at microscopic to macroscopic length scales.

### 2.2. Direct ink writing

The first example of a ceramic component printed using direct ink writing and a preceramic polymer was published by Pierin et al. in 2016 [34], where we demonstrated that a silicone resin solution could possess a suitable Herschel-Bulkley rheology, enabling the fabrication of SiOC scaffolds (for that specific preceramic polymer (MK, Wacker Chemie, Germany). The rheology could be further improved by the addition of cross-linked particles of the same material). Additional work was carried out to fabricate SiOC components with tunable porosity by adding sacrificial fillers (PMMA microbeads) to a preceramic polymer ink (MK,

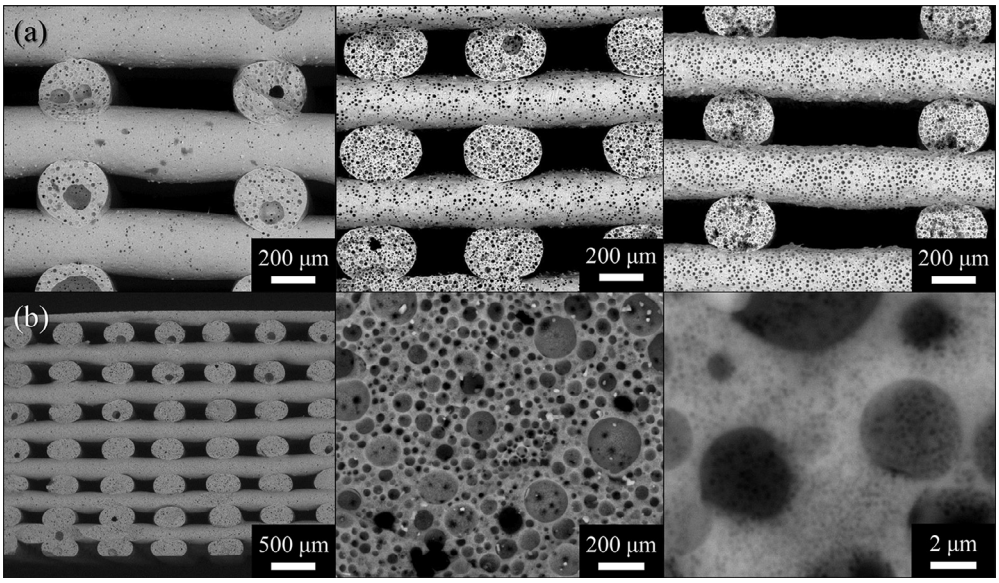


**Fig. 5.** SEM images of: (a) SiOC pyrolyzed porous scaffolds printed by DIW, derived from the removal of different amounts of PMMA particles (50 vol.%, 60 vol.%, 80 vol.%, respectively); (b) a SiOC scaffold with a hierarchical pore structure obtained by combining PMMA particles with different nominal size (25 μm and 0.46 μm).

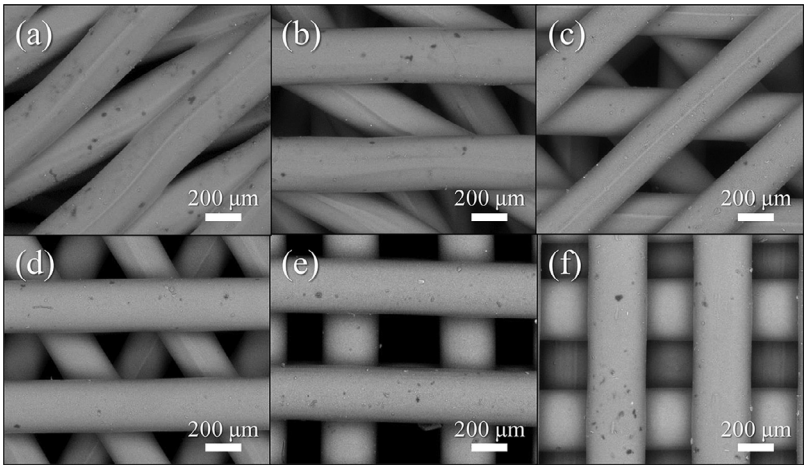


**Fig. 6.** Pyrolyzed SiOC scaffolds with different angles of deflection: (a)15°, (b) 30°, (c) 45°, (d) 60°, (e)90°) and (f) a SiOC scaffold with a shifted architecture, printed by DIW.

Wacker Chemie, Germany). By varying the filler dimensions in the range of 0.46–50 μm nominal size and the filler content from 50 to 80 vol.%, it was possible to obtain scaffolds possessing hierarchical porosity constituted by a) the designed mm-sized macro-porosity, which is controlled by the size and arrangement of the filaments in space, and b) the μm-sized porosity within the struts, provided by the elimination of the sacrificial fillers upon pyrolysis. When a suitable amount of fillers is present, which depends on the filler size, a fully interconnected porosity can be achieved within the strut cross-section as well as their surface, significantly increasing the geometric surface available for the interaction between the solid scaffold and surrounding environment. Furthermore, by mixing fillers of different sizes within the same preceramic ink, hierarchical porosity within the struts was produced [35]. Such morphological features (see Fig. 5) are of great relevance for several applications such as filtration or catalyst supports.

The following study was conducted using a different preceramic polymer, which is a solventless, two-part silicone adhesive (DOWSIL™ SE 1700, Dow, USA). The rheology of this precursor proved suitable for the fabrication of scaffolds with very complex geometries based on a log-pile structure in which every layer was rotated by a certain angle (15°, 30°, 45°, 60°, and 90°) with respect to the previous one or was shifted by a distance equal to the strut size (see Fig. 6). Mechanical tests and permeability measurements enabled the connection between the morphology of the scaffolds and their performance, demonstrating that it was possible to print ceramic components with an architecture that maximized the desired properties for a specific application. Compression strength values as high as ~130 MPa were obtained for the scaffolds produced using a 200 μm nozzle, 100 μm filament spacing, and ~52 vol.% porosity, and the gas permeability was in the range of that of the ceramic foams produced by the replica technique for samples with a total porosity of ~65 vol.% [36].

Because this specific two-part silicone adhesive (DOWSIL™ SE 1700) is an elastomer, we successfully exploited its flexibility for the manufacturing of SiOC components with very complex architectures, starting from 2D sheets of various geometries assembled (before pyrolysis) into 3D structures using the origami technique (see Fig. 7). This approach is very versatile because folding at very sharp angles did not lead to any damage to the silicone material, even after pyrolysis. The folded structures could retain the shape given by folding either using a filament based on the same preceramic polymer or, more advantageously, by self-adhesion in the unpyrolyzed state, which was controlled by the degree of crosslinking achieved within the material [37]. Therefore, no metallic filaments were used to avoid the unfolding of the structures during pyrolysis, as in a previous study [38]. Moreover, using this approach, it is also possible to fabricate a component that contains moving parts, something that would not be possible to obtain with DIW technology.

Direct ink writing is a very versatile technology possessing some advantages with respect to digital light processing because concentrated

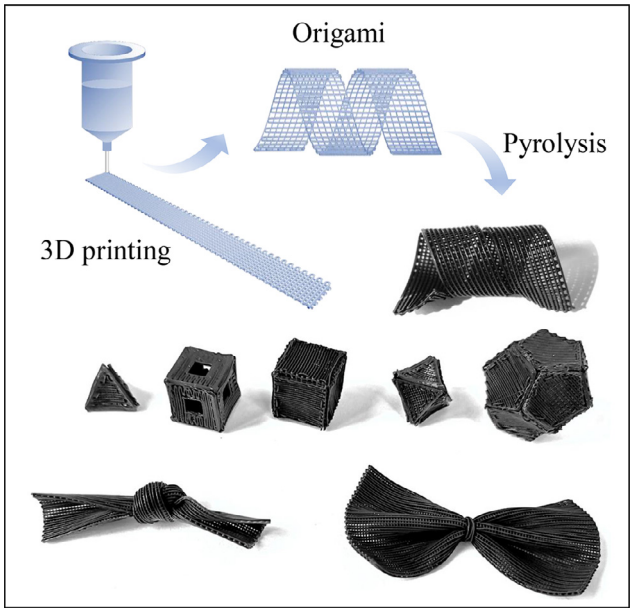


**Fig. 7.** Complex 3D SiOC structures, after pyrolysis, fabricated by direct ink writing and origami using a silicone elastomer.

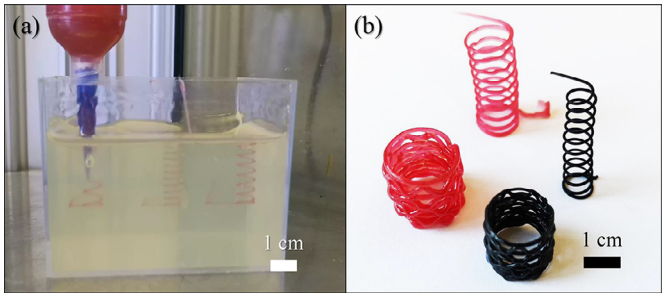


**Fig. 8.** (a) Digital image of the E-DIW process and (b) printed and pyrolyzed SiOC structures with suspended features.

solutions/slurries can be used and the printing envelope is generally much larger. However, it also has disadvantages such as the larger minimum feature size achievable, the lower the surface quality of the parts, and more significantly, a limitation in terms of the shapes that can be achieved because of the requirement for the printing nozzle to follow a continuous path (unless a very efficient control of the gas pressure in the printing head is implemented). Therefore, inspired by the hydrogel AM literature, we developed, concurrently and independently from another research group [39], an embedded direct ink writing (E-DIW) approach that overcomes some of the intrinsic limitations of the technology, enabling the use of a larger range of ink formulations without requiring the strict control of their rheology. Using an ink based on a dissolved silicone resin (MK, Wacker Chemie, Germany) and a vat containing vegetable oil and colloidal silica, we successfully printed structures at very steep angles and with great shape freedom (free-forming) without sacrificial supports (see Fig. 8) [40].

Pursuing the same aim of enabling free-form printing, we also implemented a UV-assisted direct ink writing (UV-DIW) process that employs a photocurable, transparent preceramic ink that enables fast and complete curing of the extruded filament upon exit from the nozzle. In contrast with the published literature where the only existing example is that of a structure that could have been fabricated by conventional DIW [41], we successfully printed print free-standing structures without any additional support (see Fig. 9). Furthermore, by carefully controlling the viscosity and reactivity of the ink, we manufactured structures with very

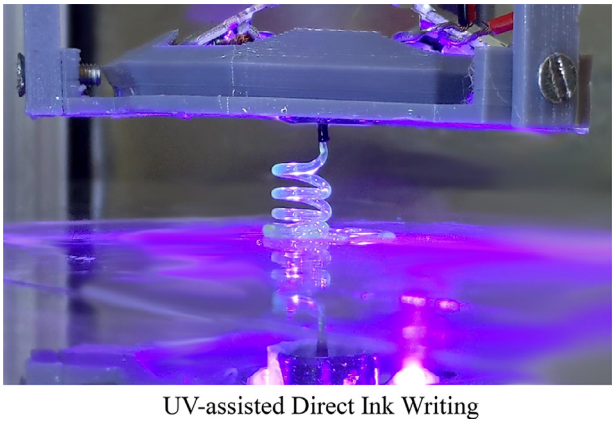


**Fig. 9.** Preceramic coil being printed using the DIW+UV process.

fine details that could not be obtained using conventional preceramic ink because of the necessary and strict requirements for its rheology in terms of the yield stress and pseudoplastic behavior.

Finally, using appropriate preceramic feedstocks, such as a silicone elastomer (DOWSIL$^{TM}$ SE 1700, Dow, USA), it was possible to fabricate structures by DIW or UV-DIW using a six-axis robotic arm, providing an additional degree of shaping freedom with respect to conventional printers based on a delta or Cartesian configuration [42].

A summary of all the preceramic polymer-based feedstocks and AM technologies tested so far is presented in Table 2 [26-31,34-37,42]. It should be noted that the minimum strut thickness reported may be an indication of technology resolution but also depends on the chosen geometry and application.

## 3. Geopolymer-based Feedstocks

A geopolymer is an amorphous aluminosilicate network synthesized via the dissolution of an aluminosilicate source (such as calcined kaolin, fly ash, waste glass, or red mud) in a highly alkaline (or rarely highly acidic) environment, followed by condensation into an amorphous 3D-network. Because the dissolution of the initial aluminosilicate powder in the first stage of the reaction is usually quite fast, the resulting slurry can be considered an all-liquid system during the additive process. Upon dissolution, alumina and silica tetrahedra are present as free monomers; their accumulation induces them to rearrange in a gel of secondary tetrahedral rings, which then develop into polymer-like chains, and finally into a solid, interconnected 3D-network. The reaction can take a few minutes to a few hours and occurs at room temperature, although it can be accelerated by mild heating (<120°C) [43].

### 3.1. Direct ink writing

Owing to their chemical nature, geopolymer slurries are ideal candidates for material extrusion AM processes, namely, DIW. In fact, the condensation reaction produces a physical gel of molecules with an increase in size over time, which provides intrinsic shear-thinning behavior, which is a key factor for allowing the extrusion of the slurry and retention of the shape of the printed component. Room-temperature consolidation and fast setting allow for the fabrication of net-shaped components without post-processing or thermal treatment.

We were the first to exploit geopolymer network formation for the fabrication of porous lattices using DIW [45]. We demonstrated the shear-thinning nature of the Na-based geopolymer slurries (molar composition: $SiO_2/Al_2O_3$=3.8, $Na_2O/Al_2O_3$=1, $H_2O/Na_2O$ = 13, and 13.78); however, the formation of a geopolymer network in the initial stages was too weak to provide sufficient shape retention upon extrusion. A suitable ink for DIW was achieved with the addition of 5 wt%

**Table 2**
Preceramic polymer and AM technology combinations presented, with details on resulting resolution and behavior upon pyrolysis.

| Preceramic polymer-based feedstock | Supplier | AM family | Technology | Min. strut thickness (after pyrolysis) ($\mu$m) | Pyrolysis linear Shrinkage (%) | Ceramic yield (wt%) | Reference |
|---|---|---|---|---|---|---|---|
| Silicone resin (MK) + silane acrylate (TMPSM) | Wacker Chemie Sigma | Vat photopolymerization | DLP | ~200 | ~25 | ~70 | [26] |
| Silicone resins (H44 and Silres 601) + silicone acrylate (TEGO RC 711) | Wacker Chemie Evonik Industries | | DLP | ~30 (RC 711) 58 (RC 711/601 = 1/1) 49 (RC 711/H44 = 1/1) | 70.1 ± 0.5 (pure RC 711) 42.4 ± 3.8 (RC 711/601 = 1/1) 51.4 ± 3.3 (RC 711/H44 = 1/1) | 7.4 (pure RC 711) 47.6 (RC 711/601 = 3/7) 60.2 (RC 711/H44 = 3/7) | [27,28] |
| Silicone resin (H44) + organic photocurable resin | Wacker Chemie Fun To Do | | DLP | ~1500 | ~30 | ~27 | [29] |
| Silicone acrylate (TEGO RC 711) | | | TPP | 0.45 | 51 - 56, depending on the geometry | 7.4 | [30] [31] |
| Evonik Industries | | | DLP+TPP | | 70.4 | | |
| Silicone resin (H44) + organic photocurable resin | Evonik Industries Xolo GmbH | | Xolography | 150 | 40 - 60 | 10 - 40 | unpublished work |
| Silicone resin (MK) | Wacker Chemie | Material extrusion | DIW E-DIW | 119 ± 1 | ~20 | up to ~67, depending on the amount of solvent (16-40 wt%) | [34–36] |
| Silicone elastomer (DOWSIL SE 1700) | Dow | | DIW R-DIW | ~300 | 25 - 37, depending on the geometry | 72.5 | [37,42] |
| Silicone resin (H44) + organic photocurable resin | Wacker Chemie Fun To Do | Hybrid | UV-DIW | 150 | ~25 | ~50 | unpublished work |

of polyethyleneglycole (PEG), which provided a higher initial viscosity, higher elastic modulus, wider working window, and faster viscosity recovery after extrusion. Using the optimized ink, we fabricated lattices with more than 70 vol.% porosity and suspended struts with very limited sagging (7% of the deposited filament diameter).

The condensation of the alternating silica and alumina tetrahedra into a 3D-network also results in an intrinsically mesoporous structure. It is worth noting that the composition of a geopolymer is similar to that of a zeolite; particularly, it can be considered as its amorphous counterpart. The combination of geopolymers and DIW allows for the fabrication of components with hierarchical porosity, with channels and macropores provided by the process, and mesopores provided by the material. This feature, together with the room-temperature consolidation and the possibility of employing waste materials as the aluminosilicate source, makes geopolymers an affordable and sustainable alternative for application as sorbents and catalysts.

We tested lattice structures with the same composition as that described previously [45] for the removal of ammonium ions from wastewater [46]. Geopolymers have a high affinity for cations such as $NH^{4+}$, which can be effectively exchanged with charge-balancing $Na^+$ cations in the aluminosilicate network. Accessibility to the charge-bearing sites is guaranteed by the material mesoporosity as well as the chosen design, a log-pile structure with 45° stacking possessing continuous yet tortuous channels, and non-stochastic open porosity of approximately 49 %vol. The resulting components showed higher permeability and lower resistance to flow compared to state-of-the-art granular and powdered activated carbon with the same porosity, as well as a high removal efficiency (≥80% after multiple cycles) with no visible damage.

The modification of geopolymer materials with metals can also be performed to add antimicrobial functionality to the sorbents [47]. In this work, we evaluated different alternatives for the incorporation of Ag and Cu into the lattices: the addition of metal salts or nanoparticles to the fresh paste, dipping into a colloidal solution, and ion-exchange (substitution of $Na^+$ in the network with $Ag^+/Cu^{2+}$ ions). Using the first two manufacturing methods, we detected minimal leaching and met the drinking water guidelines. The most promising filters will be tested in disinfection and advanced oxidation processes (AOPs) for water treatment.

Unmodified geopolymers can also be directly used as catalysts. Alkali metal cations ($Na^+$, $K^+$, $Cs^+$, and others) are often involved in catalytic reactions, and a good example of a well-established industrial process is the transesterification of triglycerides into biodiesel, typically catalyzed by a strong alkali alcoholic solution. The catalyst is in the liquid phase (i.e., homogeneous catalysis) and becomes soluble in the final reaction mixture; therefore, it is very difficult to separate it from biodiesel and reuse it.

We demonstrated that sodium- and potassium-based geopolymers can act as heterogeneous catalysts because of their charge-bearing cations [48], and evaluated the efficiency of 3D printed lattice structures [49,50]. After 6 h of reactions, the biodiesel conversion yield was between 70% and 85% for all compositions, lower than that of conventional homogeneous catalysts (>95%) but similar to that reported for many powders and resins (80%–95%) [51].

Lattice geopolymer catalysts require very mild reaction conditions (temperature and methanol:oil ratio); because of their mechanical properties and permeability, they can be used directly in bench-top fixed-bed reactors and do not require any separation step, thus saving cost and operating time.

The combination of the process-induced macroporosity, intrinsic mesoporosity, and ion exchange capabilities of geopolymers processed by DIW also suggests their use as a carrier structure for biocatalysts. Particularly, the cation exchange to $NH^{4+}$ allows for surface functionalization with $NH_2$ groups, facilitating the immobilization process by the covalent bonding of enzymes such as Candida rugosa lipase. We used Na-based geopolymer lattices functionalized with lipase for enzymatic hydrolysis to process biodiesel from waste cooking oil [52], resulting in a biodiesel yield of 75%. Owing to the strong interaction between the enzyme and geopolymer, its activity remained higher than 91% after the first reuse. This is a promising result in terms of reusability and stability in low-cost reagents, such as waste cooking oil.

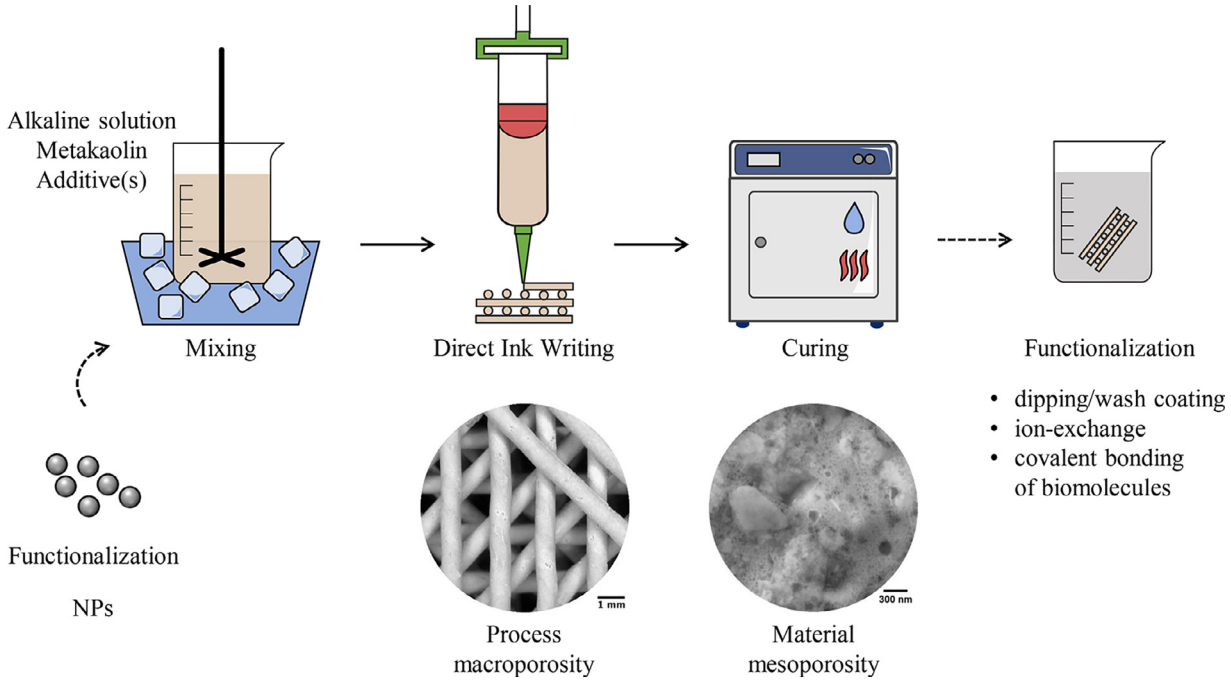


**Fig. 10.** Schematic of the production process of geopolymer components: mixing, direct ink writing, curing (up to 120°C). The fabrication process provides for the macro-porosity of the components, the material itself for its meso-porosity. Different functionalization options are available before and after fabrication.

A schematic of the AM process for geopolymer components is shown in Fig. 10, highlighting the different functionalization options presented in this paragraph. Optical microscopy and SEM images provide typical examples of the macro- and meso-porosity of the as-produced components.

## 4. Sol-gel-based Feedstocks

Among the all-liquid ceramic AM approaches, sol-gel-based feedstocks provide the highest versatility in terms of the final ceramic composition, with typical precursors being metal alkoxides or metal salts that undergo hydrolysis and condensation to form a colloid of either discrete particles or polymer chain networks. It is possible to tailor the chemical and physical properties influencing the printing processes, such as the rheology and reaction rates, by controlling several parameters, such as the temperature, pH, catalyst system, and precursor:solvent ratio. Homogeneity in multicomponent systems can be reached at the molecular scale owing to the absence of suspended powders, and is retained in the final objects, which also require lower firing temperatures compared to traditional production routes. However, the removal of a large amount of solvent usually present in sol-gel-derived wet gels is a critical step, and monolithic components are easily fractured during drying; the development of stronger, more concentrated gels could help overcome this issue.

### *4.1. Vat photopolymerization*

To the best of our knowledge, only two examples of digital light processing of sol-gel-based inks have been reported in literature. First, a hydroxyl-group-containing methacrylate was added to the sol-gel precursor solution to functionalize the forming network, enabling photopolymerization reactions [53]. Second, the photocurable moiety was provided by a hybrid organic-inorganic polymer participating in the network as a glass source [54].

In this work, we propose the physical blending of a photocurable polymer with a sol-gel precursor solution, similar to what has already been validated with preceramic polymer solutions. In this approach, no condensation reaction occurs between the two different systems, and two competing networks are formed. The choice of acrylates with high reactivity is much broader than that of the hydroxyl group-containing or hybrid organic-inorganic precursors.

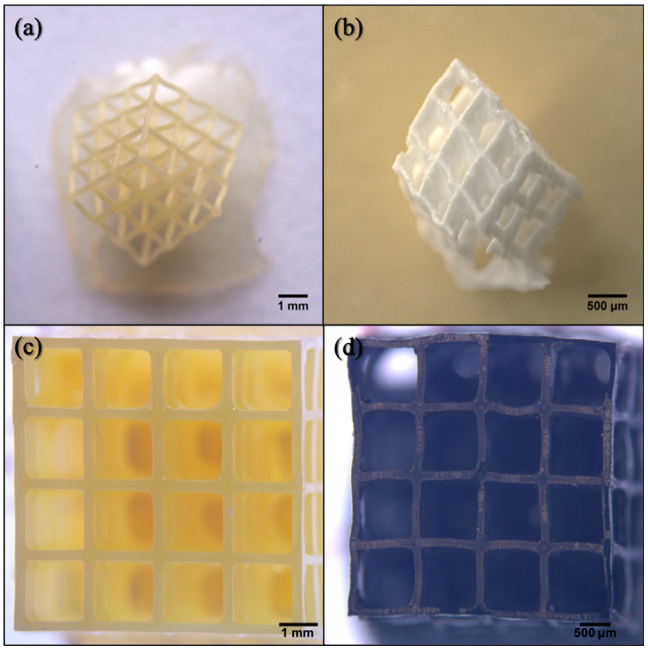


**Fig. 11.** Ceramic components from DLP of sol-gel inks: (a) $ZrO_2$ lattices after printing and (b) after sintering at 1100°C in air; (c) TiC lattices after printing and (d) after sintering at 1750°C in Ar.

As a proof-of-concept we present in Fig. 11, oxide and non-oxide components fabricated using this route.

First, we fabricated zirconia components using a photocurable sol-gel ink based on zirconium butoxide and polyethylene glycol diacrylate

(PEGDA). In this case, the organic fraction was completely removed by subsequent debinding and sintering treatments. However, the hybrid organic-inorganic nature of the feedstock can also be exploited for the synthesis of carbides through carbothermal reduction. The second example involves the development of a photocurable sol-gel system containing titanium isopropoxide and sucrose for the fabrication of microporous TiC components with a high specific surface area.

### 4.2. UV-DIW

Our recent experiments demonstrated that sol-gel photocurable inks can be adapted for the UV-DIW approach by adding a thickener to regulate the initial viscosity of the feedstock in the initial stages of the reaction.

## 5. Additional Possibilities

Despite the advantages of using a completely liquid feedstock, in some cases, it is necessary to add particles to the system to obtain ceramic parts with compositions outside those easily achievable with liquid precursors or with the aim of introducing additional functionalities, such as the possibility of achieving graceful failure upon fracture, as afforded by the presence of (chopped) fibers. Nevertheless, in these cases, the presence of a reactive or unreactive non-sacrificial liquid is beneficial, as it reduces the number of particles that it would be necessary to have in the feedstocks, leading to lower viscosity values or higher fiber loadings with respect to all-particle systems.

For example, we used powder-containing preceramic feedstocks for the fabrication of bioceramic scaffolds using the DIW technique [16,55] or mullite structures using the DLP technique [56].

In this study, for the first time, feedstocks containing chopped carbon fibers and a preceramic polymer (MK, Wacker Chemie, Germany) were used for the additive manufacturing of ceramic matrix composite (CMC) structures by direct ink writing [44,57]. This approach enabled the fabrication of composites with a fiber content of ~20 vol.%, with the fibers in the struts aligned along the printing direction owing to the shear stress generated in the nozzle.

Finally, we established an approach that does not directly rely on the additive manufacturing of liquid feedstocks but employs a preceramic solution for the replica of (conventional) polymer components. By controlling the type of polymer used, preceramic polymer formulation, soaking time, and pyrolysis process, we fabricated SiCN cellular ceramic parts that accurately reproduced the original polymeric 3D geometry [58]. Additional work was then carried out to expand the range of polymeric filaments suitable for the approach, and to obtain dense cross-sections after pyrolysis [59].

Considering the intrinsic nature of geopolymers that enable room- to low-temperature consolidation without requiring any firing, various types of fillers can be introduced without issues related to thermal decomposition, provided that they can withstand the alkaline environment of the matrix. The addition of fillers can be structural, that is, they can provide improved rheological properties to the ink, as well as lower shrinkage upon drying and eventual thermal treatments, thereby lowering the risk of cracks and breakage. We demonstrated this particularly with the addition of ground geopolymer powders of the same chemical composition as the matrix [60]; the use of the ground geopolymer is particularly beneficial for sorption and catalysis applications because it allows the increase of the amount of water in the matrix (and therefore its SSA) while preserving the workability of the ink.

Remarkably, fillers can provide additional functionality. We are currently focusing on the addition of microporous fillers, such as zeolites and activated carbons, to add one more level of porosity and specific adsorption capabilities to the printed components. The SSA of these composite components can be effectively increased, even with a low amount of filler (< 40 wt %), indicating that the filler itself remains accessible owing to the mesoporous nature of the matrix and is not damaged by the alkaline environment. Experiments on water treatment (Oliveira et al., unpublished data) and functionalization via $Cu^{2+}$ exchange [61] have shown promising results. Other researchers have evaluated printing by DIW of parts containing graphene oxide as a filler, providing electrical conductivity after annealing [62].

## 6. Conclusions and Perspectives

The additive manufacturing of ceramics from liquid feedstocks is a fast-growing field attracting the interest of several researchers across the globe, certainly because of the advantages discussed in this paper.

Particularly, the application of preceramic polymers with different AM technologies has significantly expanded, demonstrating the viability of this approach for the fabrication of Si-based ceramic components with increasingly complex architectures [3,63]. Besides our research group, several other scientists have probed and expanded the field of the additive manufacturing of preceramic polymers, working mainly on DLP [9,21,64-76], DIW [10,77,78], TPP and micro-stereolithography [79–82], using a variety of precursors. Additional attempts at the fabrication of CMCs [83–87], as well as employing FDM [88] or further exploring the replica technique to obtain fully dense cross-sections [89] have also been carried out (note: the above list of publications does not intend to be exhaustive but aims to highlight some of the more significant or earlier contributions to the literature on additive manufacturing using preceramic polymer-based feedstocks). In addition to their involvement in the fabrication of CMCs, preceramic polymers are gaining particular interest in the development of energy storage devices. Polymer-derived ceramics possess favorable electrochemical properties resulting from their unique nanodomain structure [90]. Hierarchal 3D porous components produced by AM methods may facilitate ion transport and yield higher power and energy densities owing to an increased surface area and improved electrolyte penetration, allowing easy integration of the devices with commercial products [91].

The use of geopolymer feedstocks in extrusion-based processes has also attracted significant interest because of their potential use in the building industry [92–97]. As discussed, their reactive nature can present challenges in terms of the continuous adjustment of the process parameters and a limited working window; therefore, a transition towards a continuous mixing and feeding system is foreseen. Simultaneously, more work should be conducted to find additives suitable for further controlling the rheology of the ink to enable the fabrication of parts with highly controlled geometries without sacrificing their intrinsic mesoporosity [98]. Particularly, the addition of functional fillers to geopolymer-based inks appears to be a promising route for the fabrication of components with advanced functionalities and bespoke characteristics, such as sorbents, catalyst carriers, and energy storage components. Their room-temperature consolidation also suggests the exploration of multi-material AM in combination with polymers for the fabrication of composites; they are also biocompatible if not bioactive [99,100], and could even be coupled with hydrogels and living organisms (i.e., cells, bacteria) for applications in bioengineering.

The use of sol-gel feedstocks promises to be the most versatile all-liquid AM fabrication approach because it can overcome particle sedimentation, aggregation, viscosity constraints, and light scattering with no limitations on the final composition. However, their reactivity and post-treatment requirements (particularly those related to drying), as well as the strength of the printed part, pose additional challenges compared to conventional AM. Therefore, devising specific strategies for the preparation of concentrated solutions and the use of low-volatility solvents are necessary. Moreover, their generally aqueous nature demands further exploration of hydrophilic photocurable moieties and water-soluble photoinitiators, a development that would also facilitate the use of commercial ceramic particle dispersions already employed in conventional forming processes, such as slip casting.

It is possible that the field of AM of ceramics from liquid feedstocks has now reached a sufficient degree of maturity for moving beyond the

mere fabrication of complex ceramic structures to testing their application in a wide range of advanced engineering applications, as highlighted. Furthermore, considering the ever-expanding range of available equipment and AM technologies, volumetric techniques, which can exploit and benefit from the transparency of all-liquid systems, appear to be very promising for the rapid and efficient fabrication of ceramic parts. Simultaneously, innovative hybrid manufacturing approaches, such as UV-DIW, appear to be particularly amenable for fabricating ceramic components from preceramic polymers and sol-gel systems, extending the range of geometries achievable. The use of a robotic arm for DIW or UV-DIW printing will further expand both the printing envelope and shape flexibility of the parts, ultimately allowing the fabrication of complex truss architectures with enhanced mechanical properties resulting from overcoming layer interfaces. A major focus in the coming years, shared with conventional feedstocks, is also expected to be on the refining of AM technologies towards a higher reliability and the reduction of defects and waste materials, implementing process control and management systems according to Industry 4.0 principles.

## CRediT authorship contribution statement

PC and GF devised the structure and content of the paper and wrote the bulk of the text. The other authors contributed to the preparation of the figures, revision and discussion of the literature, and completion of the manuscript. All authors read and approved the final manuscript.

## Declaration of Competing Interest

The authors declare that they have no known competing financial interests or personal relationships that could have appeared to influence the work reported in this paper.

## Acknowledgments

Dr. N. König and D. Radzinski, Xolo GmbH, Germany, are acknowledged for their contribution to the development of printable preceramic polymer feedstock. J. Schmidt acknowledges the CARIPARO Foundation, Padova, Italy for providing her PhD scholarship. K. Huang acknowledges the support from the China Scholarship Council (Grant No. 201804910741). Y. Feng acknowledges the support from the China Scholarship Council (Grant No. 201806220175). The authors are indebted to Evonik for providing the RC711 photocurable silicone. Dr. M. Braga of INGESSIL is acknowledged for supplying the sodium and potassium silicates.

## References

[1] Zocca A, Elsayed H, Bernardo E, et al. 3D-printed silicate porous bioceramics using a non-sacrificial preceramic polymer binder. Biofabrication 2015;7(2):25008. doi:10.1088/1758-5090/7/2/025008.
[2] Zocca A, Colombo P, Gomes C M, et al. Additive manufacturing of ceramics: Issues, potentialities, and opportunities. J Am Ceram Soc 2015;98(7):1983–2001. doi:10.1111/jace.13700.
[3] Rasaki S A, Xiong D, Xiong S, et al. Photopolymerization-based additive manufacturing of ceramics: a systematic review. J Adv Ceramic 2021;10(3):442–71. doi:10.1007/s40145-021-0468-z.
[4] Wang Zhen, Huang Chuanzhen, Wang Jun, et al. Development of a novel aqueous hydroxyapatite suspension for stereolithography applied to bone tissue engineering. Ceram Int 2019;45(3):3902–9. doi:10.1016/J.CERAMINT.2018.11.063.
[5] Wang Wei, Sun Jinxing, Guo Binbin, et al. Fabrication of piezoelectric nanoceramics via stereolithography of low viscous and non-aqueous suspensions. J Eur Ceram Soc 2020;40(3):682–8. doi:10.1016/J.JEURCERAMSOC.2019.10.033.
[6] Zheng T, Wang W, Sun J, et al. Development and evaluation of $Al_2O_3$–$ZrO_2$ composite processed by digital light 3D printing. Ceram Int 2020;46(7):8682–8. doi:10.1016/J.CERAMINT.2019.12.102.
[7] Chen Z, Li J, Liu C, et al. Preparation of high solid loading and low viscosity ceramic slurries for photopolymerization-based 3D printing. Ceram Int 2019;45(9):11549–57. doi:10.1016/J.CERAMINT.2019.03.024.
[8] Li Xingbang, Zhong He, Zhang Jingxian. Fabrication of zirconia all-ceramic crown via DLP-based stereolithography. Int J Appl Ceram Technol 2020;17(3):844–53. doi:10.1111/IJAC.13441.
[9] Li Ziyong, Chen Zhangwei, Liu Jian, et al. Additive manufacturing of lightweight and high-strength polymer-derived SiOC ceramics. Virtual Phys Prototyp 2020;15(2):163–77. doi:10.1080/17452759.2019.1710919.
[10] Fu Shengyang, Liu Wei, Liu Shiwei, et al. 3D printed porous $\beta$-$Ca_2SiO_4$ scaffolds derived from preceramic resin and their physicochemical and biological properties. Sci Technol Adv Mater 2018;19(1):495–506. doi:10.1080/14686996.2018.1471653.
[11] P F Jacobs. Rapid prototyping & manufacturing: fundamentals of stereolithography. Dearborn, MI: Society of Manufacturing Engineers in cooperation with the Computer and Automated Systems Association of SME,1992.
[12] Colombo P, Mera G, Riedel R, et al. Polymer-derived ceramics: 40 years of research and innovation in advanced ceramics. Ceramic Sci Technol Appl 2013;4(7):245–320. doi:10.1002/9783527631971.ch07.
[13] He Rujie, Zhou Niping, Zhang Keqiang, et al. Progress and challenges towards additive manufacturing of SiC ceramic. J Adv Ceramic 2021;10(4):637–74. doi:10.1007/s40145-021-0484-z.
[14] Zocca A, Gomes C M, Staude A, et al. SiOC ceramics with ordered porosity by 3D-printing of a preceramic polymer. J Mater Res 2013;28(17):2243–52. doi:10.1557/jmr.2013.129.
[15] Zocca A, Gomes C, Linow U, et al. Structural optimization of printed structures by self-organized relaxation. Rapid Prototyp J 2016;22(2):344–9. doi:10.1108/RPJ-07-2014-0087.
[16] Zocca A, Franchin G, Elsayed H, et al. Direct ink writing of a preceramic polymer and fillers to produce hardystonite ($Ca_2ZnSi_2O_7$) bioceramic scaffolds. J Am Ceram Soc 2016;99(6):1960–7. doi:10.1111/jace.14213.
[17] Gorjan L, Tonello R, Sebastian T, et al. Fused deposition modeling of mullite structures from a preceramic polymer and $\gamma$-alumina. J Eur Ceram Soc 2019;39(7):2463–71. doi:10.1016/j.jeurceramsoc.2019.02.032.
[18] Abbatinali E, Caminero M A, García-Plaza E, et al. Additive manufacturing of dense mullite structures using fused deposition modeling (FDM). J Eur Ceram Soc 2021;41:6677–86.
[19] Chen J, Wang Y, Pei X, et al. Preparation and stereolithography of SiC ceramic precursor with high photosensitivity and ceramic yield. Ceram Int 2020;46(9):13066–72. doi:10.1016/j.ceramint.2020.02.077.
[20] Eckel Z C, Zhou C Y, Martin J H, et al. Additive manufacturing of polymer-derived ceramics. Science 2016;351(6268):58–62. doi:10.1126/science.aad2688.
[21] Hundley J M, Eckel Z C, Schueller E, et al. Geometric characterization of additively manufactured polymer derived ceramics. Addit Manuf 2017;18:95–102. doi:10.1016/j.addma.2017.08.009.
[22] Cui H, Hensleigh R, Chen H, et al. Additive Manufacturing and size-dependent mechanical properties of three-dimensional microarchitected, high-temperature ceramic metamaterials. J Mater Res 2018;33(3):360–71. doi:10.1557/jmr.2018.11.
[23] Wang Xifan, Schmidt F, Hanaora D, et al. Additive manufacturing of ceramics from preceramic polymers: a versatile stereolithographic approach assisted by thiol-ene click chemistry. Addit Manuf 2019;27:80–90. doi:10.1016/j.addma.2019.02.012.
[24] de Hazan Y, Penner D. SiC and SiOC ceramic articles produced by stereolithography of acrylate modified polycarbosilane systems. J Eur Ceram Soc 2017;37(16):5205–12. doi:10.1016/j.jeurceramsoc.2017.03.021.
[25] He Chong, Ma Cong, Li Xilu, et al. Polymer-derived SiOC ceramic lattice with thick struts prepared by digital light processing. Addit Manuf 2020;35:101366. doi:10.1016/j.addma.2020.101366.
[26] Zanchetta E, Cattaldo M, Franchin G. Stereolithography of SiOC Ceramic Microcomponents. Adv Mater 2016;28(2):370–6. doi:10.1002/adma.201503470.
[27] Schmidt J, Colombo P. Digital light processing of ceramic components from polysiloxanes. J Eur Ceram Soc 2018;38(1):57–66. doi:10.1016/j.jeurceramsoc.2017.07.033.
[28] Brodnik N R, Schmidt J, Colombo P, et al. Analysis of multi-scale mechanical properties of ceramic trusses prepared from preceramic polymers. Addit Manuf 2020;31:10095. doi:10.1016/j.addma.2019.100957.
[29] Feng Yurun, Guo Xue, Huang Kai, et al. Enhanced electromagnetic microwave absorption of SiOC ceramics targeting the integration of structure and function. J Eur Ceram Soc 2021;41(13):6393–405. doi:10.1016/j.jeurceramsoc.2021.06.007.
[30] Brigo L, Schmidt J E M, Gandin A, et al. 3D nanofabrication of SiOC ceramic structures. Adv Sci 2018;5(12):180937. doi:10.1002/advs.201800937.
[31] Schmidt J, Brigo L, Gandin A, et al. Multiscale ceramic components from preceramic polymers by hybridization of vat polymerization-based technologies. Addit Manuf 2019;30:100913. doi:10.1016/j.addma.2019.100913.
[32] Kelly B, Bhattacharya I, Heidari H, et al. Volumetric additive manufacturing via tomographic reconstruction. Science 2019;363(6431):1075–9. doi:10.1126/SCIENCE.AAU7114/SUPPL_FILE/AAU7114S5.MOV.
[33] Regehly M, Garmshausen Y, Reuter M, et al. Xolography for linear volumetric 3D printing. Nature 2020;588(7839):620–4. doi:10.1038/s41586-020-3029-7.
[34] Pierin G, Grotta C, Colombo P, et al. Direct ink writing of micrometric SiOC ceramic structures using a preceramic polymer. J Eur Ceram Soc 2016;36(7):1589–94. doi:10.1016/j.jeurceramsoc.2016.01.047.
[35] Huang K, Elsayed H, Franchin G, et al. 3D printing of polymer-derived SiOC with hierarchical and tunable porosity. Addit Manuf 2020;36:10154. doi:10.1016/j.addma.2020.101549.
[36] Huang K, Elsayed H, Franchin G, et al. Complex SiOC ceramics from 2D structures by 3D printing and origami. Addit Manuf 2020;33:10114. doi:10.1016/j.addma.2020.101144.
[37] Huang K, Elsayed H, Franchin G, et al. Additive manufacturing of SiOC scaffolds with tunable structure-performance relationship. J Eur Ceram Soc 2021;41(15):7552–9. doi:10.1016/j.jeurceramsoc.2021.08.043.
[38] Liu G, Zhao Y, Wu G, et al. Origami and 4D printing of elastomer-derived ceramic structures. Sci Adv 2018;4(8):641–58. doi:10.1126/sciadv.aat0641.

[39] Mahmoudi M, Wang Chao, Moreno S, al et. Three-dimensional printing of ceramics through “carving” a gel and “filling in” the precursor polymer. ACS Appl Mater Interfaces 2020;12(28):31984–91. doi:10.1021/acsami.0c08260.
[40] Huang K, Elsayed H, Franchin G, et al. Embedded direct ink writing of freeform ceramic components. Appl Mater. Today 2021;23:101005. doi:10.1016/j.apmt.2021.101005.
[41] Wei Lai, Li Jing, Zhang Shuai, et al. Fabrication of SiOC ceramic with cellular structure via UV-Assisted direct ink writing. Ceram Int 2020;46(3):3637–43. doi:10.1016/j.ceramint.2019.10.083.
[42] Biasetto L, Franchinb G, Elsayed H, et al. Direct Ink Writing of cylindrical lattice structures: a proof of concept. Open Ceramics 2021;7:100139. doi:10.1016/j.oceram.2021.100139.
[43] Sotelo-Piña C, Aguilera-González E N, Martínez-Luévanos A. Geopolymers: past, present, and future of low carbon footprint eco-materials. *Handbook Ecomaterial* Springer 2018. doi:10.1007/978-3-319-48281-1_54-1.
[44] Franchin G, Wahl L, Colombo P. Direct ink writing of ceramic matrix composite structures. J Am Ceram Soc 2017;100(10):4397–401. doi:10.1111/jace.15045.
[45] Franchin G, Scanferla P, Zeffiro L, al et. Direct ink writing of geopolymeric inks. J Eur Ceram Soc 2017;37(6):2481–9. doi:10.1016/j.jeurceramsoc.2017.01.030.
[46] Franchin G, Pesonen J, Luukkonen T, et al. Removal of ammonium from wastewater with geopolymer sorbents fabricated via additive manufacturing. Mater Des 2020;195:109006. doi:10.1016/j.matdes.2020.109006.
[47] Luukkonen T, Yliniemi J, Sreenivasan H, et al. Ag- or Cu-modified geopolymer filters for water treatment manufactured by 3D printing, direct foaming, or granulation. Sci Rep 2020;10(1):1–14. doi:10.1038/s41598-020-64228-5.
[48] Botti R F, Innocentini M D M, Faleiros TA, et al. Biodiesel processing using sodium and potassium geopolymer powders as heterogeneous catalysts. Molecules 2020;25(12):2839. doi:10.3390/molecules25122839.
[49] Innocentini M D M, Botti R F, Bassi P M, al et. Lattice-shaped geopolymer catalyst for biodiesel synthesis fabricated by additive manufacturing. Ceram Int 2019;45(1):1443–6. doi:10.1016/j.ceramint.2018.09.239.
[50] Bottia R F, Innocentinib M D M, Faleiros T A, et al. Additively manufactured geopolymer structured heterogeneous catalysts for biodiesel production. Appl Mater Today 2021;23:101022. doi:10.1016/j.apmt.2021.101022.
[51] Ramos M, Dias A P S, Puna J F, et al. Biodiesel production processes and sustainable raw materials. Energies 2019;12(23):4408. doi:10.3390/en12234408.
[52] Santos L K, Botti R F, D de M Innocentinic M. 3D printed geopolymer: an efficient support for immobilization of Candida rugosa lipase. Chem Eng J 2021;414:128843. doi:10.1016/j.cej.2021.128843.
[53] Rosental T, Mizrahi S, Kamyshny A, al et. Particle-free compositions for printing dense 3D ceramic structures by digital light processing. Virt Phys Prototyp 2021;16(3):255–66. doi:10.1080/17452759.2021.1922121.
[54] Cooperstein I, Shukrun E, Press O, et al. Additive manufacturing of transparent silica glass from solutions. ACS Appl Mater Interfaces 2018;10(22):18879–85. doi:10.1021/acsami.8b03766.
[55] Elsayed H, Rebesan P, Crovace M C, et al. Biosilicate® scaffolds produced by 3D-printing and direct foaming using preceramic polymers. J Am Ceram Soc 2019;102(3):1010–20. doi:10.1111/jace.15948.
[56] Schmidt J, Altun A A, Schwentenwein M, et al. Complex mullite structures fabricated via digital light processing of a preceramic polysiloxane with active alumina fillers. J Eur Ceram Soc 2019;39(4):1336–43. doi:10.1016/j.jeurceramsoc.2018.11.038.
[57] Franchin G, Maden H S, Wahl L, et al. Optimization and characterization of preceramic inks for direct ink writing of ceramic matrix composite structures. Materials 2018;11(4):1–14. doi:10.3390/ma11040515.
[58] Jana P, Santoliquido O, Ortona A, al et. Polymer-derived SiCN cellular structures from replica of 3D printed lattices. J Am Ceram Soc 2018;101(7):2732–8. doi:10.1111/jace.15533.
[59] Kulkarni A, Sorarù G D, Pearce J M. Polymer-derived SiOC replica of material extrusion-based 3-D printed plastics. Addit Manuf 2020;32:100988. doi:10.1016/j.addma.2019.100988.
[60] Scanferla P, Conte A, Sin A, et al. The effect of fillers on the fresh and hardened properties of 3D printed geopolymer lattices. Open Ceramics 2021;6:100134. doi:10.1016/j.oceram.2021.100134.
[61] Cepollaro E M, Cimino S, Lisi L, al et. Cu-exchanged 3D-printed geopolymer/ZSM-5 monolith for selective catalytic reduction of NOx. *Chem Eng Trans*. Italian Assoc Chem Eng - AIDIC 2021;84:67–72. doi:10.3303/CET2184012.
[62] Zhong J, Zhou GX, He PG. 3D printing strong and conductive geo-polymer nanocomposite structures modified by graphene oxide. Carbon 2017;117:421–6. doi:10.1016/j.carbon.2017.02.102.
[63] Zhou S, Mei H, Chang P, et al. Molecule editable 3D printed polymer-derived ceramics. Coord Chem Rev 2020;422:213486. doi:10.1016/j.ccr.2020.213486.
[64] Brinckmann S A, Patra N, Yao J, al et. Stereolithography of SiOC polymer-derived ceramics filled with SiC Micronwhiskers. Adv Eng Mater 2018;20(11):1800593. doi:10.1002/adem.201800593.
[65] Fu Yuelong, Xu Gang, Chen Zhangwei. Multiple metals doped polymer-derived SiOC ceramics for 3D printing. Ceram Int 2018;44(10):11030–8. doi:10.1016/j.ceramint.2018.03.075.
[66] Li Shan, Duan Wenyan, Zhao Tong. The fabrication of SiBCN ceramic components from preceramic polymers by digital light processing (DLP) 3D printing technology. J Eur Ceram Soc 2018;38(14):4597–603 Elsevier. doi:10.1016/j.jeurceramsoc.2018.06.046.
[67] Xu Xiaobo, Li Peiying, Ge Chunhua. 3D printing of complex-type SiOC ceramics derived from liquid photosensitive resin. ChemistrySelect 2019;4(23):6862–9. doi:10.1002/slct.201900993.
[68] Gyak K W, Vishwakarma N K, Hwang Y H, et al. 3D-printed monolithic SiCN ceramic microreactors from a photocurable preceramic resin for the high temperature ammonia cracking process. React Chem Eng 2019;4(8):1393–9. doi:10.1039/c9re00201d.
[69] He Rujie, Ding Guojiao, Zhang Keqiang, et al. Fabrication of SiC ceramic architectures using stereolithography combined with precursor infiltration and pyrolysis. Ceram Int 2019;45(11):14006–14. doi:10.1016/j.ceramint.2019.04.100.
[70] Wang Min, Xie Chen, He Rujie, et al. Polymer-derived silicon nitride ceramics by digital light processing based additive manufacturing. J Am Ceram Soc 2019;102(9):5117–26. doi:10.1111/jace.16389.
[71] Xiao Jun, Liu Dongqing, Cheng Haifeng, et al. Carbon nanotubes as light absorbers in digital light processing three-dimensional printing of SiCN ceramics from preceramic polysilazane. Ceram Int 2020;46(11):19393–400. doi:10.1016/j.ceramint.2020.04.282.
[72] Xiao Jun, Jia Yan, Liu Dongqing, et al. Three-dimensional printing of SiCN ceramic matrix composites from preceramic polysilazane by digital light processing. Ceram Int 2020;46(16):25802–7. doi:10.1016/j.ceramint.2020.07.061.
[73] Ma Cong, He Chong, Wang Weilin, et al. Metal-doped polymer-derived SiOC composites with inorganic metal salt as the metal source by digital light processing 3D printing. Virtual Phys Prototyp 2020;15(3):294–306. doi:10.1080/17452759.2020.1752967.
[74] Al-Ajrash S M N, Browning C, Eckerle R, et al. Initial development of preceramic polymer formulations for additive manufacturing. Mater Adv 2021;2(3):1083–9. doi:10.1039/d0ma00742k.
[75] He Chong, Liu Xiner, Ma Cong, et al. Digital light processing fabrication of mullite component derived from preceramic precusor using photosensitive hydroxysiloxane as the matrix and alumina nanoparticles as the filler. J Eur Ceram Soc 2021;41(11):5570–7. doi:10.1016/j.jeurceramsoc.2021.04.051.
[76] He Chong, Ma Cong, Li Xilu, et al. Continuous fast 3D printing of SiOC ceramic components. Addit Manuf 2021;46:102111. doi:10.1016/j.addma.2021.102111.
[77] Larson C M, Choi J J, Gallardo P A, et al. Direct ink writing of silicon carbide for microwave optics. Adv Eng Mater 2016;18(1):39–45. doi:10.1002/adem.201500298.
[78] Chen H, Wang X, Xue F, et al. 3D printing of SiC ceramic: Direct ink writing with a solution of preceramic polymers. J Eur Ceram Soc 2018;38(16):5294–300. doi:10.1016/j.jeurceramsoc.2018.08.009.
[79] Pham T A, Kim D, Park S H, et al. Three-dimensional SiCN ceramic microstructures via nano-stereolithography of inorganic polymer photoresists. Adv Funct Mater 2006;16(9):1235–41. doi:10.1002/adfm.200600009.
[80] Park S, Lee D H, Ryoo H I, et al. Fabrication of three-dimensional SiC ceramic microstructures with near-zero shrinkage via dual crosslinking induced stereolithography. Chem Commun 2009;32:4880–2. doi:10.1039/b907923h.
[81] Bauer J, Crook C, Izard AG, et al. Additive manufacturing of ductile, ultrastrong polymer-derived nanoceramics. Matter 2019;1(6):1547–56. doi:10.1016/j.matt.2019.09.009.
[82] Konstantinou G, Kakkava E, Hagelüken L, al et. Additive micro-manufacturing of crack-free PDCs by two-photon polymerization of a single, low-shrinkage preceramic resin. Addit Manuf 2020;35:101343. doi:10.1016/j.addma.2020.101343.
[83] Xiong Huiwen, Chen Hehao, Zhao Lianzhong, et al. SiCw/SiC p reinforced 3D-SiC ceramics using direct ink writing of polycarbosilane-based solution: microstructure, composition and mechanical properties. J Eur Ceram Soc 2019;39(8):2648–57. doi:10.1016/j.jeurceramsoc.2019.02.045.
[84] Xiong Huiwen, Zhao Lianzhong, Chen Hehao, et al. 3D SiC containing uniformly dispersed, aligned SiC whiskers: printability, microstructure and mechanical properties. J Alloys Compd 2019;809:151824. doi:10.1016/j.jallcom.2019.151824.
[85] Li Shan, Zhang Yubei, Zhao Tong, et al. Additive manufacturing of SiBCN/Si3N4w composites from preceramic polymers by digital light processing. RSC Adv 2020;10(10):5681–9. doi:10.1039/c9ra09598e.
[86] Kemp J W, Diaz A A, Malek E C. Direct ink writing of ZrB2-SiC chopped fiber ceramic composites. Addit Manuf 2021;44:102049. doi:10.1016/j.addma.2021.102049.
[87] Yang Jinhua, Yu Ran, Li Xinpan, et al. Silicon carbide whiskers reinforced SiOC ceramics through digital light processing 3D printing technology. Ceram Int 2021;47(13):18314–22. doi:10.1016/j.ceramint.2021.03.152.
[88] Zhao L, Wang X, Xiong H, et al. Optimized preceramic polymer for 3D structured ceramics via fused deposition modeling. J Eur Ceram Soc 2021;41(10):5066–74. doi:10.1016/j.jeurceramsoc.2021.03.061.
[89] Kulkarni A, Pearce J, Yang Y, et al. SiOC(N) cellular structures with dense struts by integrating fused filament fabrication 3D printing with polymer-derived ceramics. Adv Eng Mater 2021:2100535. doi:10.1002/adem.202100535.
[90] Mujib S B, Singh G. Polymer derived SiOC and SiCN ceramics for electrochemical energy storage: a perspective. Int J Ceramic Eng Sci 2021:10108. doi:10.1002/CES2.10108.
[91] Soares D, Ren Z, Mujib S B, et al. Additive manufacturing of electrochemical energy storage systems electrodes. Adv Energy Sustain Res 2021;2(5):2000111. doi:10.1002/AESR.202000111.
[92] Zhang D W, Wang D M, Lin X Q, et al. The study of the structure rebuilding and yield stress of 3D printing geopolymer pastes. Constr Build Mater 2018;184:575–80. doi:10.1016/j.conbuildmat.2018.06.233.
[93] Ma Guowei, Li Zhijian, Wang Li. Micro-cable reinforced geopolymer composite for extrusion-based 3D printing. Mater Lett 2019;235:144–7. doi:10.1016/j.matlet.2018.09.159.
[94] Panda B, Unluer C, Tan M J. Extrusion and rheology characterization of geopolymer nanocomposites used in 3D printing. Compos Part B 2019;176:107290. doi:10.1016/j.compositesb.2019.107290.
[95] Chougan M, Ghaffar S H, Jahanzat M, al et. The influence of nano-additives in strengthening mechanical performance of 3D printed multi-

binder geopolymer composites. Constr Build Mater 2020;250:118928. doi:10.1016/j.conbuildmat.2020.118928.
[96] Archez J, Texier-Mandoki N, Bourbon X. Shaping of geopolymer composites by 3D printing. J Build Eng 2021;34:101894. doi:10.1016/j.jobe.2020.101894.
[97] Archez J, Maitenaz S, Demont L, et al. Strategy to shape, on a half-meter scale, a geopolymer composite structure by additive manufacturing. Open Ceramics 2021;5:100071. doi:10.1016/j.oceram.2021.100071.
[98] Ma Siqi, Fu Shuai, Zhao Shengjian, et al. Direct ink writing of geopolymer with high spatial resolution and tunable mechanical properties. Addit Manuf 2021;46:102202. doi:10.1016/j.addma.2021.102202.
[99] Michelina C, Flavia B, Isabella L, et al. Chemical and biological characterization of geopolymers for potential application as hard tissue prostheses. Adv Sci Technol 2010;69:192–7. doi:10.4028/www.scientific.net/ast.69.192.
[100] Pangdaeng S, Sata V, Aguiar J B, et al. Bioactivity enhancement of calcined kaolin geopolymer with $CaCl_2$ treatment. ScienceAsia 2016;42(6):407–14. doi:10.2306/SCIENCEASIA1513-1874.2016.42.407.